



Article

Effect of Drying Temperature on the Physicochemical, Functional, and Microstructural Properties of Powders from *Agave angustifolia* Haw and *Agave rhodacantha* Trel

Francisco Erik González-Jiménez ¹, José Eduardo Barojas-Zavaleta ¹, Guadalupe Vivar-Vera ¹, Audry Peredo-Lovillo ¹, Alfredo Alberto Morales-Tapia ¹, Josué Antonio Del Ángel-Zumaya ¹, Mónica Reyes-Reyes ², Liliana Alamilla-Beltrán ³, Diana Elizabeth Leyva-Daniel ³ and Jaime Jiménez-Guzmán ^{1,*}

¹ Facultad de Ciencias Químicas, Universidad Veracruzana, Oriente 6 No. 1009, Rafael Alvarado, C.P. Orizaba, Veracruz 94340, Mexico

² Universidad Tecnológica de la Sierra Sur de Oaxaca, Magnolias S/N, San Idelfonso Sola, C.P. Villa Sola de Vega, Oaxaca 71400, Mexico

³ Escuela Nacional de Ciencias Biológicas, Instituto Politécnico Nacional, Wilfrido Massieu S/N UP Adolfo López Mateos, C.P., Gustavo A. Madero, Ciudad de Mexico 07738, Mexico

* Correspondence: jajimenez@uv.mx; Tel.: +52-272-7240120



Citation: González-Jiménez, F.E.; Barojas-Zavaleta, J.E.; Vivar-Vera, G.; Peredo-Lovillo, A.; Morales-Tapia, A.A.; Del Ángel-Zumaya, J.A.; Reyes-Reyes, M.; Alamilla-Beltrán, L.; Leyva-Daniel, D.E.; Jiménez-Guzmán, J. Effect of Drying Temperature on the Physicochemical, Functional, and Microstructural Properties of Powders from *Agave angustifolia* Haw and *Agave rhodacantha* Trel. *Horticulturae* **2022**, *8*, 1070. <https://doi.org/10.3390/horticulturae8111070>

Academic Editors: Romas Mažeika and Juozas Lanauskas

Received: 23 October 2022

Accepted: 4 November 2022

Published: 14 November 2022

Publisher's Note: MDPI stays neutral with regard to jurisdictional claims in published maps and institutional affiliations.



Copyright: © 2022 by the authors. Licensee MDPI, Basel, Switzerland. This article is an open access article distributed under the terms and conditions of the Creative Commons Attribution (CC BY) license (<https://creativecommons.org/licenses/by/4.0/>).

Abstract: The present study evaluated the effect of convective drying on the physicochemical, functional, and microstructural properties of the powders of leaves of *Agave angustifolia* Haw (agave espadin) and *Agave rhodacantha* Trel (agave mexicano) at temperatures of 70, 90, and 110 °C. The leaves correspond to the agro-industrial waste generated by the mezcal industry. The results indicate that convective drying at a temperature of 110 °C induces the greatest microstructural modification of the powders and improves their functional properties compared to thermal treatments at 70 and 90 °C. The obtained powders in the present investigation show important contents of dietary fiber in a range of 45.53 ± 0.07 to 55.31 ± 1.60 g/100 g. According to the results of physicochemical analysis, the obtained powders show high storage stability, pointing out that the employment of convective drying in the processing of agave leaves at high temperatures is an emerging tool for the obtention of waste-derived powders with high impact in the development of future functional foods, while contributing to the mitigation of the environmental impact of the mezcal industry.

Keywords: agro-industrial waste; convective drying; dietary fiber; SEM

1. Introduction

Several investigations focused on the analysis and study of various agro-industrial wastes to find alternatives that result in their use and exploitation. Many of these residues constitute important functional compounds such as dietary fibers, antioxidants, and phenolic compounds [1]. In this context, the growing demand for products derived from the mezcal industry potentiated the generation of agro-industrial wastes, which increase year after year. As a result, there is an increase in the production of *Agave angustifolia* Haw and *Agave rhodacantha* Trel, known in the Mexican territory commonly as “maguey espadin” and “maguey mexicano”, respectively, and recognized as two of the most agave species used in the sector to produce mezcal in Mexico. Unfortunately, during the production of this alcoholic beverage, only the heart (piña) of the agave plant (40–50%) is used. The leaves (50–60% of the plant) are left in the crop fields, creating an environmental problem due to the corrosion of the soils generated by the waste [2]. According to the agri-food and fisheries information service, in 2020 there was an agricultural production of 393,604.65 tons of mezcal agave in Mexico, which generated around 196,802.32 tons of waste (agave leaves) and, thus, a serious environmental problem. For this reason, it is of great importance to develop new alternatives for the use of these agro-industrial residues in order to mitigate the environmental problem generated by the mezcal sector.

The increasing risk of chronic degenerative diseases such as cancer, diabetes, and high blood pressure represent other current problems closely related to poor food habits that affect children and adults equally. Thus, there is an interest in developing functional ingredients that contribute to preventing and treating these diseases [3]. In the group of functional ingredients of interest are the dietary fibers whose intake is related to a low risk of colon cancer, as well as to hypotensive, anti-obesogenic, and antidiabetic effects [4]. Total dietary fiber (TDF) is constituted of carbohydrates such as cellulose, hemicellulose, pectin, and lignin, as well as intracellular polysaccharides such as gums and mucilages. It is divided into insoluble dietary fiber (IDF) and soluble dietary fiber (SDF); each show different functional properties that lead to the prevention and treatment of different metabolic disorders in the host [5].

Agave angustifolia Haw and *Agave rhodacantha* Trel leaves provide an alternative for the development of functional ingredients constituted of different phytochemical compounds of interest for the food industry, including IDF and SDF, as well as secondary metabolites characteristic of these vegetables.

This research evaluated the physicochemical, functional, and microstructural properties of powders obtained from *Agave angustifolia* Haw and *Agave rhodacantha* Trel leaves through convective drying.

2. Materials and Methods

The materials used in this study were leaves of *Agave angustifolia* Haw and *Agave rhodacantha* Trel from El Trapiche, Santa Cruz Mixtepec (16°47' N, 96°53' W; elevation 1560 masl) in Oaxaca, Mexico.

2.1. Agave Leaf Drying

Leaves were dried in a convective dryer with forced convection (Intertecnica, SA, Mexico) and a constant air speed of 1.25 m/s at 70, 90, and 110 °C. The drying times established for *Agave angustifolia* Haw leaves were 690, 210, and 150 min at 70, 90, and 110 °C, respectively. Those for *Agave rhodacantha* Trel leaves were 720, 270, and 210 at the same temperatures.

2.2. Milling

The dried leaves were milled with a commercial Oster blender. The obtained powders were passed through sieves with mesh numbers 20 and 30 with the support of a sieve shaker (W.S. Tyler Rx-812 RX-812) and were kept under shaking for 15 min to obtain a fine powder with a particle size < 595 µm [6]. The obtained powders from *Agave angustifolia* Haw leaves (AHP) were identified as AH70 (70 °C), AH90 (90 °C), and AH110 (110 °C), while those from *Agave rhodacantha* Trel (ARP) were identified as AR70 (70 °C), AR90 (90 °C), and AR110 (110 °C).

2.3. Chemical Composition

The contents of moisture (method 925.09), fat (method 983.23), protein (method 950.48), and ash (method 930.05) were evaluated according to the official methods established by AOAC [7]. Soluble (SDF) and insoluble (IDF) dietary fiber were identified according to the enzymatic–gravimetric method (985.29) established by AOAC [7]. Total dietary fiber (TDF) was established from the sum of SDF and IDF.

2.4. Physicochemical Analysis

2.4.1. Water Activity (Aw)

The water activity (Aw) of the powders was determined using a digital hygrometer (Lab-Master-aw, Lanchen, Switzerland) at 25 °C.

2.4.2. Colorimetric Analysis

The color measurement of the samples was carried out according to the CIELAB system. The parameters L*, a*, and b* were identified using a colorimeter (Konica Minolta CR-400).

The metric chroma value (Chroma*) and the metric hue angle ($^{\circ}$ Hue) were evaluated according to Equations (1) and (2) [8]:

$$\text{Chroma}^* = \sqrt{a^{*2} + b^{*2}} \quad (1)$$

$$^{\circ}\text{Hue} = \arctan\left(\frac{b^*}{a^*}\right) \quad (2)$$

2.5. Functional Properties

2.5.1. Water Solubility Index (WSI)

The water solubility index (WSI) was identified according to the technique described by Shuen et al. [9], with slight modifications. Distilled water (30 mL) was added and mixed with the leaf powders (0.3 g). The mix was shaken in a vortex mixer (Cole-Parmer™) for 30 s and placed in a water bath at 30 °C for 30 min. The suspensions were then centrifuged (Centrificient IV CRM Globe) at 3500 × g for 10 min. The supernatants were transferred to porcelain capsules at a constant weight and were dried at 105 °C for 24 h. The calculation was carried out using Equation (3):

$$\text{WSI} (\%) = \frac{\text{Weight of dissolved solids supernatant (g)} \times (V)}{\text{Sample weight (g)}} \times 100 \quad (3)$$

2.5.2. Water Absorption Capacity (WAC) and Oil Absorption Capacity (OAC)

The powder (2 g) was mixed with 20 mL distilled water/oil (corn vegetable oil) and shaken in a vortex mixer (Cole-Parmer™) for 1 min. The mix was then centrifuged (Centrificient IV CRM Globe) at 3000 × g for 30 min. Finally, the results were expressed as grams of water/oil retained per gram of sample [10].

2.5.3. Swelling Power (SP)

The swelling power of agave powders was evaluated through the methodology described by Gómez-Ordóñez et al. [11]. Briefly, 100 mg of powder was placed into a 10 mL graduated cylinder, then 10 mL of distilled water was added. The mixture was left to stand for 16 h at room temperature. After that time, the volume occupied by the powder was measured. The results were expressed in mL/g of powder.

2.5.4. Emulsifying Capacity (EC)

The emulsifying capacity of the powders was determined according to the method described by López-Marcos et al. [12], with slight modifications. A total of 20 mL of distilled water was mixed with 1 g of powder and stirred with the help of a Vortex for 15 min. After the stirring time, 5 mL distilled water and 25 mL of corn oil were added to the mixture. The resulting suspension was mixed for 5 min and finally centrifuged (Centrificient IV CRM Globe) at 1300 × g for 5 min. The results were expressed as percentage of emulsified layer.

2.6. Flow Properties

The bulk density (ρ_{bulk}) was evaluated by measuring the mass occupied by the powder (3 g) in a 10 mL measuring cylinder; it was reported as g/cm³. The packed density (ρ_{packed}) was determined by tapping the cylinder containing the powder mass on a flat surface until a constant volume was obtained. It was calculated from the proportion of mass powder and the volume occupied in the cylinder (g/cm³) [13]. Bulk (ρ_{bulk}) and packed (ρ_{packed}) densities were used to calculate the Carr index (CI) and Hausner ratio (HR), according to the following equations [14]:

$$\text{CI} (\%) = \frac{\rho_{\text{packed}} - \rho_{\text{bulk}}}{\rho_{\text{packed}}} \times 100 \quad (4)$$

$$HR = \frac{\rho_{\text{packed}}}{\rho_{\text{bulk}}} \quad (5)$$

2.7. Hygroscopicity

Hygroscopicity was identified according to the methodology proposed by Juarez-Enriquez et al. [15], with slight modifications. The powder (2 g, M_S) was added to a container with a saturated NaCl solution (75.29% relative humidity) at 25 °C; the mix was weighed 7 days after (M_{EH}). The hygroscopicity capacity of the powders was calculated according to the following equation:

$$\text{Hygroscopicity (\%)} = \frac{M_{EH} - M_S}{M_{EH}} \times 100 \quad (6)$$

2.8. Scanning Electron Microscopy (SEM)

The analysis was carried out in a scanning electron microscope (LSM 710 NLO, Carl Zeiss, Jena, Germany). The powders were mounted on an aluminum stub using double-sided carbon tape. The samples were coated with gold using a sputter electrode. The analysis was carried out at 3.0 kV using a secondary electron detector.

2.9. Statistical Analysis

The results obtained were processed using Minitab 18 software (Minitab Inc., State College, PA, USA). All determinations were performed in triplicate. The analysis of variance (ANOVA) and mean comparison were performed through Tukey's test with a confidence of 95% and a significance level of 5%.

3. Results

3.1. Physicochemical Analysis and Chemical Composition

The results of the physicochemical analysis and the chemical composition of the powders from both varieties of agave and from the different thermal treatments are presented in Table 1. According to the results obtained, AHP and ARP present low contents of humidity, ranging from 6.1 ± 0.1 to 6.5 ± 0.1 g/100 g and 6.5 ± 0.1 to 6.6 ± 0.2 g/100 g, respectively. Regarding the water activity, the AHP and ARP powders show values ranging from 0.34 ± 0.02 to 0.46 ± 0.01 and 0.25 ± 0.00 to 0.41 ± 0.00 , respectively. The AH110 sample presents the highest Aw value (0.46 ± 0.01) and is significantly higher than the Aw value found in the AR110 sample (0.25 ± 0.00).

Table 1. Physicochemical composition of *Agave angustifolia* Haw and *Agave rhodacantha* Trel leaf powders.

Parameters (g/100 g) *	AHP			ARP		
	AH70	AH90	AH110	AR70	AR90	AR110
Moisture *	6.5 ± 0.1^a	6.4 ± 0.0^{ab}	6.1 ± 0.1^b	6.6 ± 0.2^a	6.5 ± 0.1^a	6.5 ± 0.1^a
Aw	0.37 ± 0.03^{bc}	0.34 ± 0.02^c	0.46 ± 0.01^a	0.40 ± 0.00^b	0.41 ± 0.00^b	0.25 ± 0.00^d
Ash *	14.37 ± 0.31^a	14.49 ± 0.09^a	13.82 ± 0.85^a	13.36 ± 0.29^a	14.28 ± 0.43^a	12.07 ± 0.03^b
Fat *	2.07 ± 0.35^c	4.39 ± 0.13^{ab}	4.45 ± 0.25^{ab}	1.63 ± 0.26^c	3.82 ± 0.33^b	4.96 ± 0.26^a
Proteins *	3.46 ± 0.01^c	3.42 ± 0.04^c	3.38 ± 0.01^c	8.54 ± 0.12^b	13.08 ± 0.16^a	12.99 ± 0.07^a
IDF *	37.33 ± 0.61^a	32.20 ± 0.38^b	25.52 ± 0.01^d	26.29 ± 0.24^d	26.04 ± 0.22^d	29.79 ± 0.45^c
SDF *	12.17 ± 1.51^d	21.07 ± 1.69^c	29.79 ± 1.61^a	19.24 ± 0.28^c	25.86 ± 0.67^b	22.16 ± 0.68^c
TDF *	49.50 ± 1.86^b	53.27 ± 1.47^{ab}	55.31 ± 1.60^a	45.53 ± 0.07^c	51.90 ± 0.54^b	51.95 ± 0.52^b

Mean \pm SD; $n = 3$. Different letters indicate significantly difference ($p \leq 0.05$) between means in the same row. AHP = *Agave angustifolia* Haw leaf powders; AH70 = sample dried at 70 °C; AH90 = sample dried at 90 °C; AH110 = sample dried at 110 °C; ARP = *Agave rhodacantha* Trel leaf powders; AR70 = sample dried at 70 °C; AR90 = sample dried at 90 °C; AR110 = sample dried at 110 °C. Aw = water activity; IDF = insoluble dietary fiber; SDF = soluble dietary fiber; TDF = total dietary fiber. * Units indicator.

In relation to the lipid content of the analyzed powders, the samples AH110 and AR110 present the highest lipid contents (4.45 ± 0.25 and 4.96 ± 0.26 g/100 g, respectively),

while the AH70 and AR70 samples exhibit the lowest lipid contents with 2.07 ± 0.35 and 1.63 ± 0.26 g/100 g, respectively. When evaluating the effect of temperature on the lipid content of the powders, a proportional relationship is found; that is, the higher the drying temperature, the higher the lipid content. The lower lipid content in AH70 and AR70 could be associated with the prolonged drying times (690 and 720 min, respectively) to which these samples were subjected, since, on average, the time is four times greater than the time of drying for samples AH110 and AR110, in which the highest lipid content is observed.

In relation to the protein content present in the powders (Table 1), the values obtained for the AHP samples ranges between 3.38 ± 0.01 and 3.46 ± 0.01 g/100 g, and are significantly ($p \leq 0.05$) lower than the values found in the ARP samples whose protein contents ranges from 8.54 ± 0.12 to 13.08 ± 0.16 g/100 g.

The obtained powders from both varieties of agave and from the different thermal treatments show similar mineral (ash) content, presenting values in a range from 12.07 ± 0.03 to 14.49 ± 0.09 g/100 g.

According to the analysis of TDF, the obtained powders in the present investigation present high levels of dietary fiber. The TDF content ranges between 45.53 ± 0.07 and 55.31 ± 1.60 g/100 g; the samples AR70 and AH110 present the lowest and the highest TDF content, respectively. However, the IDF content is higher than the SDF content present in the powders, except for sample AH110, where the SDF fraction (29.79 ± 1.61 g/100 g) is higher than that of IDF (25.52 ± 0.01 g/100 g). Likewise, samples AH70 and AH90 present the highest IDF contents compared to the other samples analyzed with 37.33 ± 0.61 and 32.20 ± 0.38 g/100 g, respectively. Regarding the content of SDF, the samples dried at 70°C (AH70 and AR70) present the lowest contents with respect to the samples treated at a higher drying temperature.

Color is a major parameter for quality control in the food industry because it is a key feature for a good perception of food; it is also relevant to a good sensory acceptance of the product. Therefore, it is important to evaluate the effect of temperature on the color of the obtained powders for their possible application as additives in different food systems, without damaging the color perception of the final product. The values of the parameters of the colorimetric analysis are presented in Table 2, in which luminosity (L^*), a^* , b^* , Chroma*, and $^\circ\text{Hue}$ values are presented. Interestingly, for AHP and ARP samples treated at 110°C and for the sample ARP treated at 90°C , the values obtained correspond to darker powders, compared to those obtained in lower drying temperatures. As for the values of the coordinate a^* , the samples show negative values, except for sample AR90, which indicates that AR90 presents reddish tones. In contrast, the rest of the samples (AH70, AH90, AH110, AR70, and AR110) present negative values for the b^* coordinate, which indicates that the samples present slight shades of green. On the other hand, the values obtained for b^* are positive in the analysis of each of the samples. This indicates that the samples tend to yellow. According to the color parameters of metric Chroma* and the metric $^\circ\text{Hue}$ angle, samples AH110 and AR110 show a dark yellow color, while those obtained from thermal treatments at 70 and 90°C (AH70, AH90, AR70, and AR90) are light yellow.

Table 2. Colorimetric analysis of *Agave angustifolia* Haw and *Agave rhodacantha* Trel leaf powders.

Parameters	AHP			ARP		
	AH70	AH90	AH110	AR70	AR90	AR110
L^*	62.78 ± 1.44^a	63.87 ± 0.46^a	58.76 ± 1.73^b	64.60 ± 0.37^a	53.55 ± 0.25^c	58.83 ± 0.42^b
A^*	-1.77 ± 0.05^c	-2.12 ± 0.04^d	-0.30 ± 0.16^b	-2.31 ± 0.06^d	2.70 ± 0.07^a	-1.55 ± 0.05^c
B^*	23.30 ± 0.3^c	26.57 ± 0.29^a	21.58 ± 0.74^d	25.27 ± 0.07^b	23.47 ± 0.37^c	23.49 ± 0.10^c
Chroma*	23.36 ± 0.29^c	26.65 ± 0.29^a	21.58 ± 0.74^d	25.37 ± 0.08^b	23.62 ± 0.36^c	23.54 ± 0.10^c
$^\circ\text{Hue}$	85.64 ± 0.19^{bc}	85.43 ± 0.03^c	89.21 ± 0.39^a	84.77 ± 0.13^d	83.43 ± 0.27^e	86.22 ± 0.10^b

Mean \pm SD; $n = 3$. Different letters indicate significantly difference ($p \leq 0.05$) between means in the same row. AHP = *Agave angustifolia* Haw leaf powders; AH70 = sample dried at 70°C ; AH90 = sample dried at 90°C ; AH110 = sample dried at 110°C ; ARP = *Agave rhodacantha* Trel leaf powders; AR70 = sample dried at 70°C ; AR90 = sample dried at 90°C ; AR110 = sample dried at 110°C . L = luminosity; a = the red (+) or green (-) coordinate; b = the yellow (+) or blue (-) coordinate; Chroma* = chromaticity; $^\circ\text{Hue}$ = hue angle of color.

3.2. Functional Properties

The results of the evaluation of the functional properties are presented in Table 3. The results obtained in relation to the WSI for the ARP samples indicate that this property is not influenced by the drying temperature; it shows values from 5.32 ± 0.21 to $5.58 \pm 0.29\%$, significantly ($p \leq 0.05$) lower than those found in the AHP samples. In contrast, WSI in AHP is higher as the drying temperatures increase. Correlation could be associated with the inverse proportion between WSI and IDF in AHP (Table 1); that is, when the IDF content is higher, the solubility index decreases.

Table 3. Functional properties of *Agave angustifolia* Haw and *Agave rhodacantha* Trel leaf powders.

Parameters	AHP			ARP		
	AH70	AH90	AH110	AR70	AR90	AR110
WSI (%)	27.64 ± 0.48^c	29.75 ± 0.95^b	33.36 ± 1.16^a	5.32 ± 0.21^d	5.58 ± 0.29^d	5.46 ± 0.15^d
WAC (g H ₂ O/g sample)	2.64 ± 0.06^b	3.03 ± 0.11^a	3.17 ± 0.16^a	2.44 ± 0.02^{bc}	2.23 ± 0.11^c	2.38 ± 0.03^{bc}
OAC (g oil/g sample)	1.58 ± 0.02^d	2.66 ± 0.05^c	3.05 ± 0.17^b	3.27 ± 0.01^{ab}	3.16 ± 0.11^{ab}	3.41 ± 0.13^a
SP (mL/g)	4.34 ± 0.11^d	4.66 ± 0.45^d	6.04 ± 0.23^c	7.35 ± 0.15^b	8.30 ± 0.28^a	8.62 ± 0.12^a
EC (%)	3.91 ± 0.27^c	5.31 ± 0.16^b	6.32 ± 0.21^a	2.96 ± 0.32^d	3.65 ± 0.28^{cd}	4.76 ± 0.28^b

Mean \pm SD; $n = 3$. Different letters indicate significantly difference ($p \leq 0.05$) between means in the same row. AHP = *Agave angustifolia* Haw leaf powders; AH70 = sample dried at 70 °C; AH90 = sample dried at 90 °C; AH110 = sample dried at 110 °C; ARP = *Agave rhodacantha* Trel leaf powders; AR70 = sample dried at 70 °C; AR90 = sample dried at 90 °C; AR110 = sample dried at 110 °C. WSI = water solubility index; WAC = water absorption capacity; OAC = oil absorption capacity; SP = swelling power; EC = emulsifying capacity.

Looking at the WAC values, AH90 and AH110 show the highest WAC (3.03 ± 0.11 and 3.17 ± 0.16 g water/g sample, respectively), while AR90 shows the lowest values (2.23 ± 0.11 g water/g sample). Similarly, AHP samples present a proportional correlation between WAC and WSI; that is, higher WSI values correspond to higher WAC, indicating there is a favorable influence of WSI on WAC. Additionally, WAC is also affected by IDF and SDF, showing a better WAC when IDF is lower or when SDF is higher.

Regarding the oil absorption capacity (OAC) of powders, the sample AR110 presents the highest OAC (3.41 ± 0.13 g oil/g sample), while AH70 presents the lowest (1.58 ± 0.02 g oil/g sample). On average, the ARP samples exhibit better oil absorption capacity compared to the AHP samples. Likewise, the AH110 and AR110 samples exhibit a better OAC compared to the samples obtained from the treatments at 70 and 90 °C. These results can be associated with the proportional correlation between the lipid content and the OAC of samples AH110 and AR110, which possess the highest lipid contents (4.45 ± 0.25 and 4.96 ± 0.26 g/100 g, respectively).

Among functional properties, swelling power (SP) is a key indicator to evaluate when assessing DF functionality, since it is closely related to the capacity to reduce cholesterol. In addition, this provides a notion on the supplementation levels in foods to provide them with a desirable texture [16]. Table 3 shows that SP increases in the powders along with the processing temperature, and the highest value is found in samples dried at 110 °C (AH110 and AR110). They show significant differences ($p \leq 0.05$) with respect to samples treated at 70 and 90 °C. The differences between SP values found in this research could be associated with the difference in the physical structure of the powders, since this indicator is highly influenced by the porosity and crystallinity of the matrix of powders. Similar values are also observed and reported in functional DF from green and ashen bagasse [17].

3.3. Flow Properties

The flow properties of AHP and ARP are presented in Table 4. The bulk density values found in ARP oscillate between 0.75 ± 0.04 and 1.05 ± 0.01 g/cm³, respectively, and are significantly different from each other ($p \leq 0.05$). Furthermore, they present values that are significantly higher ($p \leq 0.05$) than those found in AHP.

Table 4. Flow properties of *Agave angustifolia* Haw and *Agave rhodacantha* Trel leaf powders.

Parameters	AHP			ARP		
	AH70	AH90	AH110	AR70	AR90	AR110
Bulk density (g/cm ³)	0.66 ± 0.05 ^d	0.60 ± 0.006 ^{de}	0.55 ± 0.003 ^e	1.05 ± 0.01 ^a	0.84 ± 0.01 ^b	0.75 ± 0.04 ^c
Packed density (g/cm ³)	0.77 ± 0.06 ^d	0.74 ± 0.005 ^d	0.70 ± 0.05 ^d	1.41 ± 0.03 ^a	1.16 ± 0.03 ^b	0.93 ± 0.07 ^c
CI (%)	15.47 ± 1.37 ^c	23.39 ± 2.56 ^{ab}	26.96 ± 1.85 ^a	25.50 ± 1.50 ^{ab}	27.23 ± 3.12 ^a	19.83 ± 2.02 ^{bc}
HR	1.15 ± 0.01 ^d	1.23 ± 0.02 ^{cd}	1.26 ± 0.01 ^{bc}	1.34 ± 0.02 ^{ab}	1.37 ± 0.06 ^a	1.24 ± 0.03 ^c
Hygroscopicity (%)	7.05 ± 0.09 ^b	6.52 ± 0.19 ^{cd}	6.76 ± 0.21 ^{bc}	7.60 ± 0.12 ^a	7.76 ± 0.01 ^a	6.21 ± 0.24 ^d

Mean ± SD; $n = 3$. Different letters indicate significantly difference ($p \leq 0.05$) between means in the same row. AHP = *Agave angustifolia* Haw leaf powders; AH70 = sample dried at 70 °C; AH90 = sample dried at 90 °C; AH110 = sample dried at 110 °C; ARP = *Agave rhodacantha* Trel leaf powders; AR70 = sample dried at 70 °C; AR90 = sample dried at 90 °C; AR110 = sample dried at 110 °C. CI = Carr index; HR = Hausner ratio.

It is observed that the packed density decreases as the drying temperature increases from 70 to 110 °C (Table 4). Sample AR70 presents the highest packed density (1.41 ± 0.03 g/cm³), with significant differences ($p \leq 0.05$) in comparison to the other samples analyzed. The packed density of AHP samples ranges from 0.70 ± 0.05 to 0.77 ± 0.06 g/cm³ and, according to the ANOVA performed, they show no significant differences ($p \leq 0.05$) between them.

Bulk and packed densities are parameters used collectively for the calculation of CI and HR, which indicate the flow and cohesion capacity of the powders, respectively [14]. According to the results obtained, it can be established that sample AH70 shows a good flow capacity, since it shows the lowest CI at $15.47 \pm 1.37\%$. It is followed by AR110, which presents a fair flow capacity. On the other hand, AR90 shows a poor flow capacity, while AH90 and AR70 exhibit a passable flow behavior, according to the flowability scale presented by Mishra et al. [18].

According to Gawalek et al. [19], when $HR > 1.4$, powders show high cohesion and low flow capacity. In this sense, it can be said that samples AR70 and AR90 show high cohesion between particles, thus, reducing their flow capacity. On the other hand, the HR value of sample AH70 (1.15 ± 0.01) indicates low cohesion between particles, contributing to a good flow capacity compared to the other samples analyzed.

3.4. Hygroscopicity

The hygroscopic capacity of the obtained powders is presented in Table 4. This property indicates the disposition of granular materials to absorb water vapor from the environment at a constant temperature. It largely depends on the structure of the material. The hygroscopic capacity of AHP samples ranges from 6.52 ± 0.19 to $7.05 \pm 0.09\%$; samples AH90 and AH70 show the lowest and highest hygroscopic capacity, respectively. On the other hand, samples AR70 and AR90 exhibit the greatest hygroscopic capacity (7.60 ± 0.12 and $7.76 \pm 0.01\%$, respectively), showing significant differences ($p \leq 0.05$) compared to the rest of the samples analyzed. Based on these results, the obtained powders in this study can be considered non-hygroscopic, because they show values below 10%, which can guarantee a desirable storage stability. According to Joardder et al. [20], the low hygroscopicity of the samples, as observed in AHP and ARP, can be associated with the drying method used, which, in this case, is convective drying. Convective drying creates microstructures with difficult rehydration mechanisms due to the specific low free volume in the molecular matrix. Therefore, the structures cannot incorporate large amounts of water vapor from the atmosphere.

3.5. Microstructural Analysis (SEM)

Figure 1 shows SEM images from samples AHP and ARP obtained through different thermal treatments. Comparatively, the micrographs reveal that the microstructure of the samples AHP and ARP is affected by the increase in the drying temperature. As a consequence of the thermal treatment, the samples exhibit irregular structures with irregular shapes. The samples dried at 70 °C (AH70 and AR70) show smooth surfaces with low porosity and a lower degree of cell wall fragmentation due to a low drying

temperature (70 °C), promoting low water migration and leading to a uniform material contraction [21]. On the other hand, the micrographs of the samples obtained through the thermal treatment at 90 °C (AH90 and AR90) reveal a rugged look and a high degree of cell wall segmentation, resulting from an increased drying temperature. Additionally, the micrographs of samples AH110 and AR110 show that convective drying at 110 °C leads to the formation of many microcavities on the surface of powders, due to a quick evaporation of the water in the samples [22]. The samples also present fractures in the cell walls. The microstructural changes observed in the SEM images are evidence that convective drying and the processing temperature significantly affect the final microstructure of the powders.

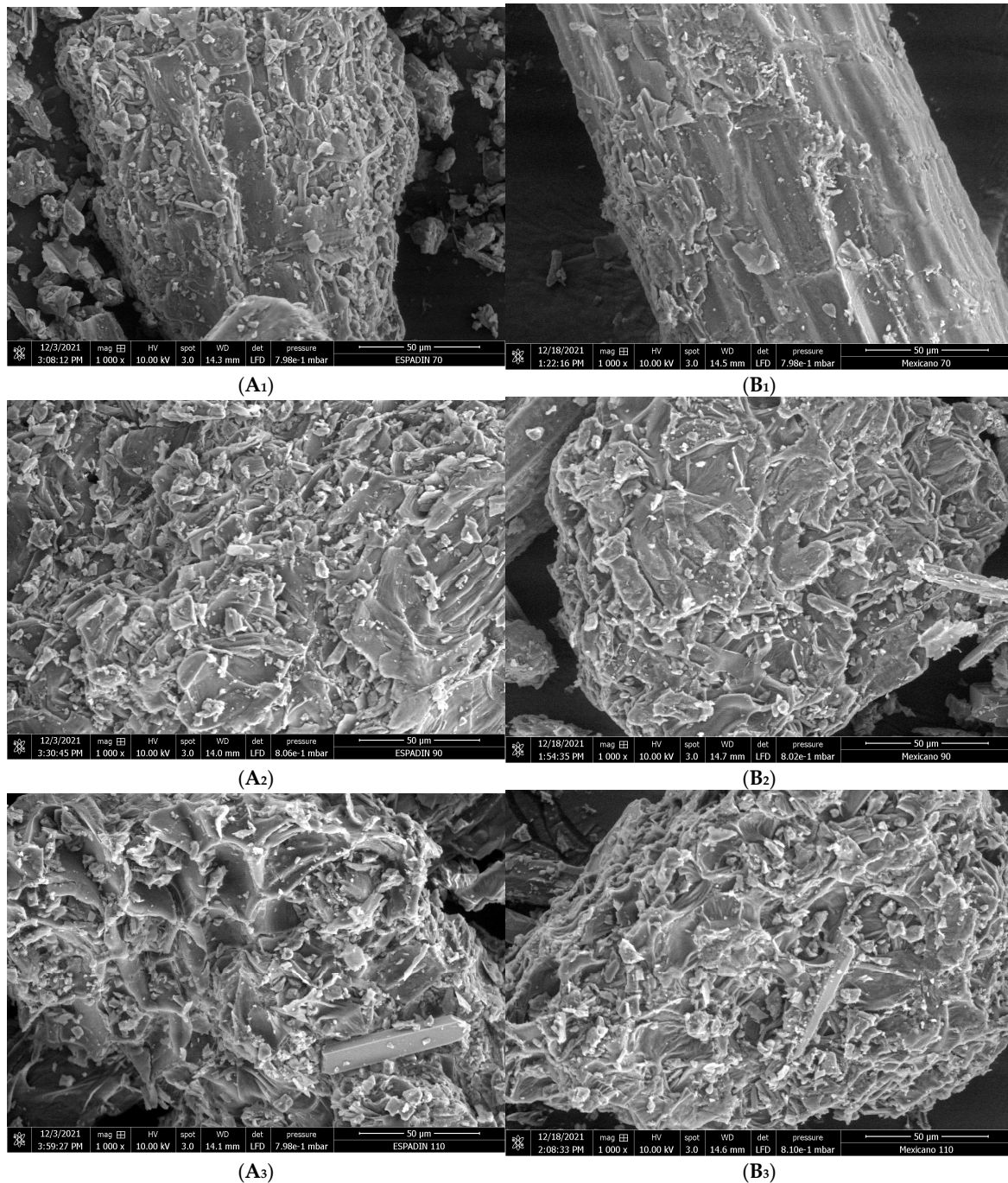


Figure 1. SEM micrographs of *Agave angustifolia* Haw and *Agave rhodacantha* Trel leaf powders. (A₁) Sample AH70; (A₂) sample AH90; (A₃) sample AH110; (B₁) sample AR70; (B₂) sample AR90; (B₃) sample AR110.

4. Discussion

The present study deals with different convective drying temperatures and their effects on the physicochemical, functional, and microstructural properties of AHP and ARP. The established drying times allow for obtaining powders with low moisture content and low A_w values (<0.6). Based on this, the dried powders emerge as functional ingredients with a potential high storage stability and microbiological security, since the A_w value does not allow for the proliferation of pathogenic or spoilage microorganisms [23]. On the other hand, the low content of lipids found in the analyzed samples may reduce the risk of oxidation and rancidification of the obtained powders, prolonging the shelf life of the powders. The lower lipid content in AH70 and AR70 could be attributed to the extended drying time (690 and 720 min, respectively) to which the samples were subjected. The protein content of the AHP samples founded in the present investigation is similar to the values reported by Jiménez-Muñoz et al. [24], who also physiochemically characterized *Agave angustifolia* Haw powders. The protein content found in the ARP samples (8.54 ± 0.12 to 13.08 ± 0.16 g/100 g) is lower than those reported by Bouaziz et al. [25], who evaluated the functional properties of powders made from *Agave americana* leaves. The ash content of AHP is slightly higher than that reported by Jiménez-Muñoz et al. [24] in the physicochemical evaluation of *Agave angustifolia* Haw leaf powder. The ash content of each of the powders analyzed in this research demonstrate important mineral levels [26], indicating the presence of essential nutrients for humans. According to the analysis, the content of TDF in the samples is inversely proportional to the drying time; that is, a longer drying time results in lower TDF. Conversely, it is proportional to the drying temperature; a higher drying temperature results in a higher TDF content. According to Ma and Mu [27], the TDF content can be affected by the method and physical obtention treatments, such as drying temperature and powdering. In the same way, several works reported TDF contents similar to those found in this work. For example, Bouaziz et al. [26] in *Agave americana* leaf powder (55.68 ± 1.47 g/100 g); Garcia-Amezquita et al. [28] in fruit peel powders from orange, mango, and fig at 49.2 ± 0.0 , 53.0 ± 1.3 , and 49.2 ± 5.6 g/100 g, respectively; and Brito et al. [23] in the processing of cabbage stalks and pineapple crowns with TDF of 42.67 ± 1.83 and 67.22 ± 1.93 g/100 g, respectively. Thus, it is established that AHP and ARP show major TDF contents, so the obtained powders in this research are a potential source of TDF and can be identified as functional ingredients with potential application in food systems. The powders mostly consist of polysaccharides such as cellulose and lignin, components of IDF that, given their functional properties, could be ideal for the development of new products rich in fiber. The content of insoluble dietary fiber and soluble dietary fiber in AHP and ARP are influenced by the effect of the drying temperature, which is associated with the fact that the application of high temperatures and the exposure for extended periods of time lead to chemical modifications, such as structural pectin hydrolysis transformed into soluble pectin, increasing SDF values, and the degradation of some SDF components. High drying temperatures can also partially degrade cellulose and hemicellulose into simpler carbohydrates, reducing IDF values [21], which modifies functional properties (WSI, WAC, OAC, SP, and SE) of DF.

The evaluation of the functional properties is of great importance, since they function as an indicator of the functionality of the powders. In the present study, the WSI of the AHP samples is influenced by the effect of the drying temperature, obtaining higher WSI values at higher drying temperatures; similar results are also reported by Garcia-Amezquita et al. [28]. On the other hand, in this research, the WSI for all the analyzed powders is considerably low. These results indicate that the obtained powders can contribute to reducing intestinal transit as well as improving the homeostasis of digestive system, generated by the low levels of WSI and the high content of insoluble dietary fiber [29]. Another property that is influenced by the effect of drying temperature is the WAC, whose values increase as the drying temperature increases in the AHP samples. Nevertheless, according to previous studies, functional properties such as WAC, can also be affected by the chemical composition of the powders (IDF and SDF content) [12]. These findings agree with what is reported by

Fuentes-Alventosa et al. [30], who indicate that the functional properties are closely related to the chemical composition of DF. The water and oil absorption capacity of samples AH110 and AR110 are similar to those reported in other investigations for meals obtained from by-products. This suggests that the powders are an alternative to be added to conventional flours. Likewise, their WAC and OAC make them potential food additives for flavor retention and improvement. In addition, the powders are potentially functional for their incorporation into products such as cold meats [31].

On the other hand, the flow properties of the agave powders are also influenced by the effect of the drying temperature, specifically the apparent density. This property presents an inversely proportional relationship with the drying temperature; that is, a lower apparent density is obtained at a higher drying temperature. This phenomenon could be attributed to the structural modification during convective drying, because the increase in drying temperature could lead to a higher degree of cell collapse, material contraction, and a faster water migration. This modification leads to a porous and fragmented structure of the food system, which alters the bulk density [32]. Consequently, the flow properties are different for each of the powders.

5. Conclusions

The present investigation establishes that the increase in the drying temperature in convective drying has an influence on the physicochemical, functional, and microstructural properties of the powders. Thus, an improvement in the functional properties and an evident microstructural modification with the increase in the drying temperature is observed. In addition, the results indicate that the agro-industrial residues generated by the mezcal sector can be used as food additives rich in dietary fiber, with important functional properties for their application in food matrices, to produce functional foods, based on their dietary fiber content. Therefore, this research provides an option for the use of agro-industrial wastes, specifically the agave leaves, that would result in the mitigation of the environmental problems generated by the mezcal sector.

Author Contributions: Writing—original draft preparation, A.A.M.-T. and J.A.D.Á.-Z.; writing—review and editing, J.J.-G., F.E.G.-J. and J.E.B.-Z.; formal analysis, M.R.-R. and D.E.L.-D.; visualization and correcting the style of the language, G.V.-V., A.P.-L. and L.A.-B. All authors have read and agreed to the published version of the manuscript.

Funding: This research received no external funding.

Institutional Review Board Statement: Not applicable.

Informed Consent Statement: Not applicable.

Data Availability Statement: The data presented in this study are available on request from the corresponding author.

Acknowledgments: To María de Jesús Perea Flores from the Center for Nanosciences and Micro and Nanotechnologies, National Polytechnic Institute for her support in the microstructural analysis.

Conflicts of Interest: The authors declare no conflict of interest.

References

1. Chaouch, M.A.; Benvenuti, S. The role of fruit by-products as bioactive compounds for intestinal health. *Foods* **2020**, *9*, 1716. [[CrossRef](#)] [[PubMed](#)]
2. Esther, M.E. Situación del Agave y sus residuos en Tamaulipas. *Rev. Energías Renov.* **2017**, *1*, 19–31.
3. Dankel, S.J.; Loenneke, J.P.; Loprinzi, P.D. Physical Activity and Diet on Quality of Life and Mortality: The Importance of Meeting One Specific or Both Behaviors. *Int. J. Cardiol.* **2016**, *202*, 328–330. [[CrossRef](#)]
4. Chen, J.; Zhao, Q.; Wang, L.; Zha, S.; Zhang, L.; Zhao, B. Physicochemical and Functional Properties of Dietary Fiber from Maca (*Lepidium meyenii* Walp.) Liquor Residue. *Carbohydr. Polym.* **2015**, *132*, 509–512. [[CrossRef](#)] [[PubMed](#)]
5. Mudgil, D.; Barak, S. Composition, Properties and Health Benefits of Indigestible Carbohydrate Polymers as Dietary Fiber: A Review. *Int. J. Biol. Macromol.* **2013**, *61*, 1–6. [[CrossRef](#)]
6. AACC 55-60.01: *Guideline for Determination of Particle Size Distribution*; AOAC: Washington, DC, USA, 2011.

7. AOAC Official Methods of Analysis of AOAC International; AOAC: Gaithersburg, MD, USA, 2005.
8. Chen, X.D. Food Drying Fundamentals. In *Drying Technologies in Food Processing*; John Wiley & Sons: Hoboken, NJ, USA, 2009; pp. 1–52.
9. Shuen, G.W.; Yi, L.Y.; Ying, T.S.; Von, G.C.Y.; Yusof, Y.A.B.; Phing, P.L. Effects of Drying Methods on the Physicochemical Properties and Antioxidant Capacity of Kuini Powder. *Braz. J. Food Technol.* **2021**, *24*, e2020086. [[CrossRef](#)]
10. Ali, A.; Wani, T.A.; Wani, I.A.; Masoodi, F.A. Comparative Study of the Physico-Chemical Properties of Rice and Corn Starches Grown in Indian Temperate Climate. *J. Saudi Soc. Agric. Sci.* **2016**, *15*, 75–82. [[CrossRef](#)]
11. Gómez-Ordóñez, E.; Jiménez-Escrig, A.; Rupérez, P. Dietary fibre and physicochemical properties of several edible seaweeds from the northwestern Spanish coast. *Food Res. Int.* **2010**, *43*, 2289–2294. [[CrossRef](#)]
12. López-Marcos, M.C.; Bailina, C.; Viuda-Martos, M.; Pérez-Alvarez, J.A.; Fernández-López, J. Properties of Dietary Fibers from Agroindustrial Coproducts as Source for Fiber-Enriched Foods. *Food Bioprocess Technol.* **2015**, *8*, 2400–2408. [[CrossRef](#)]
13. Savlak, N.; Türker, B.; Yeşilkanat, N. Effects of particle size distribution on some physical, chemical and functional properties of unripe banana flour. *Food Chem.* **2016**, *213*, 180–186. [[CrossRef](#)]
14. Bian, Q.; Sittipod, S.; Garg, A.; Ambrose, R.P.K. Bulk flow properties of hard and soft wheat flours. *J. Cereal Sci.* **2015**, *63*, 88–94. [[CrossRef](#)]
15. Juárez-Enríquez, E.; Olivas, G.I.; Zamudio-Flores, P.B.; Ortega-Rivas, E.; Pérez-Vega, S.; Sepulveda, D.R. Effect of water content on the flowability of hygroscopic powders. *J. Food Eng.* **2017**, *205*, 12–17. [[CrossRef](#)]
16. Zhu, Y.; Chu, J.; Lu, Z.; Lv, F.; Bie, X.; Zhang, C.; Zhao, H. Physicochemical and Functional Properties of Dietary Fiber from Foxtail Millet (*Setaria Italica*) Bran. *J. Cereal Sci.* **2018**, *79*, 456–461. [[CrossRef](#)]
17. Requena, M.C.; González, C.N.A.; Barragán, L.A.P.; Correia, T.; Esquivel, J.C.C.; Herrera, R.R. Functional and Physico-Chemical Properties of Six Desert-Sources of Dietary Fiber. *Food Biosci.* **2016**, *16*, 26–31. [[CrossRef](#)]
18. Mishra, M.; Kandasamy, P.; Shukla, R.N.; Kumar, A. Convective Hot-Air Drying of Green Mango: Influence of Hot Water Blanching and Chemical Pretreatments on Drying Kinetics and Physicochemical Properties of Dried Product. *Int. J. Fruit Sci.* **2021**, *21*, 732–757. [[CrossRef](#)]
19. Gawalek, J.; Domian, E.; Ryniecki, A.; Bakier, S. Effects of the Spray Drying Conditions of Chokeberry (*Aronia melanocarpa* L.) Juice Concentrate on the Physicochemical Properties of Powders. *Int. J. Food Sci. Technol.* **2017**, *52*, 1933–1941. [[CrossRef](#)]
20. Joardder, M.U.H.; Kumar, C.; Karim, M.A. Food Structure: Its Formation and Relationships with Other Properties. *Crit. Rev. Food Sci. Nutr.* **2017**, *57*, 1190–1205. [[CrossRef](#)]
21. Quispe-Fuentes, I.; Vega-Gálvez, A.; Aranda, M.; Poblete, J.; Pasten, A.; Bilbao-Sainz, C.; Wood, D.; McHugh, T.; Delporte, C. Effects of Drying Processes on Composition, Microstructure and Health Aspects from Maqui Berries. *J. Food Sci. Technol.* **2020**, *57*, 2241–2250. [[CrossRef](#)]
22. Sagar, V.R.; Suresh Kumar, P. Recent Advances in Drying and Dehydration of Fruits and Vegetables: A Review. *J. Food Sci. Technol.* **2010**, *47*, 15–26. [[CrossRef](#)]
23. Brito, T.B.N.; Pereira, A.P.A.; Pastore, G.M.; Moreira, R.F.A.; Ferreira, M.S.L.; Fai, A.E.C. Chemical Composition and Physicochemical Characterization for Cabbage and Pineapple By-Products Flour Valorization. *LWT* **2020**, *124*, 109028. [[CrossRef](#)]
24. Jiménez-Muñoz, E.; Prieto-García, F.; Prieto-Méndez, J.; Acevedo-Sandoval, O.A.; Rodríguez-Laguna, R. Caracterización físico-química de cuatro especies de agaves con potencialidad en la obtención de pulpa de celulosa para elaboración de papel. *DYNA* **2016**, *83*, 232–242. [[CrossRef](#)]
25. Bouaziz, M.A.; Bchir, B.; Chalbi, H.; Sebi, H.; Karra, S.; Smaoui, S.; Attia, H.; Besbes, S. Techno-Functional Characterization and Biological Potential of *Agave Americana* Leaves: Impact on Yoghurt Qualities. *Food Meas.* **2021**, *15*, 309–326. [[CrossRef](#)]
26. Bouaziz, M.A.; Rassaoui, R.; Besbes, S. Chemical Composition, Functional Properties, and Effect of Inulin from Tunisian *Agave Americana* L. Leaves on Textural Qualities of Pectin Gel. *J. Chem.* **2014**, *2014*, e758697. [[CrossRef](#)]
27. Ma, M.; Mu, T. Effects of Extraction Methods and Particle Size Distribution on the Structural, Physicochemical, and Functional Properties of Dietary Fiber from Deoiled Cumin. *Food Chem.* **2016**, *194*, 237–246. [[CrossRef](#)] [[PubMed](#)]
28. Garcia-Amezquita, L.E.; Tejada-Ortigoza, V.; Campanella, O.H.; Welti-Chanes, J. Influence of Drying Method on the Composition, Physicochemical Properties, and Prebiotic Potential of Dietary Fibre Concentrates from Fruit Peels. *J. Food Qual.* **2018**, *2018*, e9105237. [[CrossRef](#)]
29. Elleuch, M.; Bedigian, D.; Roiseux, O.; Besbes, S.; Blecker, C.; Attia, H. Dietary Fibre and Fibre-Rich by-Products of Food Processing: Characterisation, Technological Functionality and Commercial Applications: A Review. *Food Chem.* **2011**, *124*, 411–421. [[CrossRef](#)]
30. Fuentes-Alventosa, J.M.; Rodríguez-Gutiérrez, G.; Jaramillo-Carmona, S.; Espejo-Calvo, J.A.; Rodríguez-Arcos, R.; Fernández-Bolaños, J.; Guillén-Bejarano, R.; Jiménez-Araujo, A. Effect of Extraction Method on Chemical Composition and Functional Characteristics of High Dietary Fibre Obtained powders from Asparagus By-Products. *Food Chem.* **2009**, *113*, 665–671. [[CrossRef](#)]
31. Godswill, A.C. Proximate Composition and Functional Properties of Different Grain Flour Composites for Industrial Applications. *Int. J. Food Sci.* **2019**, *2*, 43–64. [[CrossRef](#)]
32. İzli, G.; Yildiz, G.; Berk, S.E. Quality Retention in Pumpkin Powder Dried by Combined Microwave-Convective Drying. *J. Food Sci. Technol.* **2022**, *59*, 1558–1569. [[CrossRef](#)]